

## A Dark Discharge Model of Earthquake Lightning

Shunji TAKAKI and Motoji IKEYA

Department of Earth and Space Science, Graduate School of Science, Osaka University,  
1-1 Machikaneyama, Toyonaka, Osaka 560-0043, Japan

(Received May 19, 1998; accepted for publication June 16, 1998)

A model of dark discharge in the atmosphere before a large earthquake was proposed to elucidate the mechanism of generation of earthquake lightning and related electroatmospheric phenomena. Change in seismic stress releases piezo-compensating, bound charges due to changes in the piezoelectric polarization of quartz grains in granitic rocks, which produces an intense electric field at the fault zone. The excited or ionized molecules by free electrons accelerated under the electric field produce luminous phenomena in the atmosphere. Both Maxwell and Druyvesteyn distributions of the electron energy under the induced electric field were considered to estimate the rate of ionization and excitation of  $N_2$  and  $O_2$  molecules. An electric field and spatial distribution of earthquake lightning (EQL) were calculated based on the induced charges in the piezoelectric process which accompanies an earthquake. The intensity of emission from the excitation state,  $B^3\Pi_g$  of  $N_2$  molecule was estimated at  $3 \times 10^{20}$  photons/m<sup>3</sup> close to the fault zone. A nucleus of precipitation might also be formed in a supercooled atmosphere leading to the appearance of earthquake fog and clouds.

KEYWORDS: EQL, lightning, earthquake, model, discharge, piezoelectricity, polarization, cloud

### 1. Introduction

Luminous phenomena associated with large earthquakes, which have been reported in literature for a long time, are called earthquake lightning (EQL). However, no objective data were available for scientific analysis until the Matsushiro earthquake swarm from 1965–1967. Photographs of luminous phenomena were taken in restricted areas near the epicenter.<sup>1)</sup> Reported shapes of the lightning include hemispherical light, sheet lightning and luminous cloud. The illuminance of each was estimated from the photographs. Flashes, domes of light and luminous funnels were observed just before the Kobe earthquake on January 17, 1995.<sup>2)</sup> EQL has been observed and documented since the days of the Roman Empire well before the use of electricity, although some scientists still remain skeptical and consider EQL as discharges from electric power lines.<sup>3,4)</sup>

Models for producing EQL have been proposed by several investigators<sup>3–6)</sup> following the first scientific study by Terada<sup>7)</sup> who proposed as a model (1) the electroatmospheric effect due to the streaming potential in water flow through porous rocks and soils. However, in his model, the intensity is a few orders of the magnitude too low to render it suitable to explain the occurrence of EQL. Other models include (2) luminescence from charged aerosols in the atmosphere,<sup>4)</sup> (3) strain-stimulated luminescence induced by the recombination of previously trapped electrons and holes under seismic stress<sup>5)</sup> and (4) sonoluminescence from molecular reactions in water shaken by compressional (P) waves.<sup>6)</sup> Models which consider EQL as atmospheric lightning seems convincing although the mechanism of the electric field generation has not yet been clarified.

In this paper, we propose that some EQL result from dark discharge in an atmosphere under an intense electric field induced by electric charges which appear at a fault zone. The spatial distribution and luminous intensity of EQL have been estimated considering the shift of the electron energy distribution under the electric field and the probabilities of molecular ionization and of electron attachment.

### 2. Theories of EQL

#### 2.1 Dark discharge model

Ions of atoms and molecules may be excited by recombination with an electron, but charged aerosol cannot be neutralized with the emission of visible light: the energy will be distributed to a large number of atoms constituting the aerosol particles. Sonoluminescence in water cannot explain EQL over mountains. A model of the electro-atmospheric effect due to electric potential gradients was adopted in this work to explain the photographs of EQL which occurred in the Matsushiro earthquake swarm.

There are several possible mechanisms for producing electric potential gradients; the electrokinetic phenomena associated with underground fluid flow,<sup>8)</sup> piezoelectric effect of quartz in granite<sup>3)</sup> are just two examples. The atmospheric discharge model for EQL has to be explained considering how high charge concentration can be generated and maintained in conductive earth. Piezoelectric theory had generally been discounted because the rock resistivity is too small to maintain this concentration of charges.<sup>9)</sup> However, piezoelectric effect is an attractive explanation because many crustal rocks include quartz grains which produce an intense charge density. EQL was observed over the mountains composed of quartz-diorite in the Matsushiro earthquake swarm.<sup>1)</sup> We tentatively use the piezoelectric theory to calculate electric field in the atmosphere, though new explanations for the generation of large electric potential by other mechanisms could also explain the phenomena discussed in this work.

The type of discharge in EQL is non self-sustaining if the electric field is produced by piezoelectric effects. In a discharge tube, ionization is so minimal that the ionized molecules emit no appreciable light. This mode is called the dark discharge, although a sensitive instrument would detect the emission of light from such a discharge tube. In a dark discharge model for EQL, visible emissions will be observed in the dark discharge occurring in a large sphere with a radius of about 10 to 100 m. The intensity of electric field and the shape of EQL were estimated based on this model.

2.2 Non self-sustaining discharge in the air: Maxwell and Druyvesteyn distributions

Free electrons with the density of  $4 \times 10^6 - 1 \times 10^7$  electrons  $\cdot$   $m^{-3} \cdot s^{-1}$  are generated by cosmic rays and natural radiation due to atmospheric radioactivity. The electric field generated by the seismically induced charges on the ground accelerates these electrons which ionize or excite  $N_2$  and  $O_2$  in the air. The energy levels of  $N_2$  and  $O_2$  molecules considered in this calculation are shown in Fig. 1. The excited state of  $B^3\Pi_g$  for a  $N_2$  molecule has a lifetime of 8  $\mu s$  and makes the electronic transition to the excited state of  $A^3\Sigma_u^+$  observable.<sup>10)</sup>

We calculate a relation between the seismic electric field and the ionization in the air to estimate area of luminosity. Ionization by electron impacts and the subsequent loss of free electrons through the electron attachment to  $O_2$  and  $N_2$  molecules were considered using the density of free electrons,  $n$ , in the air as

$$\frac{dn}{dt} = v_i n - v_a n + \Delta n_r, \quad (1)$$

where  $v_i$  is the ionization frequency of the molecules,  $v_a$ , the attachment frequency of electrons in dry air and  $\Delta n_r$ , the number of free electrons produced by radiation in  $1 m^3/s$ . The electron density in eq. (1) was assumed to be produced by electron-molecular collision and cosmic rays and to decay due to the attachment of electrons to the molecules.

The ionization frequency by an electron impact is described using the random velocity of electrons,  $u_e$ , as

$$v_i = N_g \int_0^\infty \Omega(u_e) u_e f(u_e) du_e, \quad (2)$$

where  $N_g$ ,  $\Omega(u_e)$  and  $f(u_e)$  are the densities of molecules for air, ionization cross section and the electron velocity distribution function, respectively. The effect of inelastic collisions of electrons with molecules was ignored in the calculation of the electron velocity distribution. The cross section,  $\Omega(E)$ , can be approximately expressed by a linear equation,  $k(E - E_i)$  as shown in Fig. 2, where  $k$  and  $E_i$  are ionization rate constant and ionization energy, respectively. This approximation is valid up to 5 eV for mean energy of electrons.<sup>11)</sup>

Maxwell and Druyvesteyn distributions are often applied to the electron energy distribution.<sup>12)</sup> Maxwell distribution,  $f_M$

is given as

$$f_M(E) = \frac{2}{\sqrt{\pi}} \left( \frac{e}{k_B T_e} \right)^{3/2} E^{1/2} \exp\left(-\frac{eE}{k_B T_e}\right), \quad (3)$$

using Boltzmann's constant,  $k_B$ , temperature of the electrons,  $T_e$  and electron charge,  $e$ . The temperature of the electrons was calculated using Langevin's mobility equation.<sup>13)</sup> An electron moves over a distance of  $\mu F$  per second, receiving a force of  $eF$ , where  $\mu$  is the mobility of electrons and  $F$ , the electric field intensity. The electron gets energy  $e\mu F^2$  per second from the electric field. The electron loses energy  $\kappa(3k_B T_e/2 - 3k_B T_g/2)$  in each collision, where  $\kappa$  and  $T_g$  are the collision loss factor and the temperature of molecules in air, respectively. The average number of collisions made by an electron in a second is  $u_e/\lambda$ , where  $\lambda$  is the mean free path of electrons. The state of  $T_e$  in equilibrium is defined by

$$e\mu F^2 = \frac{u_e}{\lambda} \kappa \frac{3}{2} k_B (T_e - T_g), \quad (4)$$

since the energy gained from the field is balanced by the elastic losses. Substituting  $u_e = [8k_B T_e / (\pi m)]^{1/2} \cdot \kappa = 2m/M$  and Langevin's mobility equation  $\mu = 0.75e\lambda / (mu_e)$ , we obtain  $T_e$  considering  $T_e \gg T_g$  as

$$T_e = 0.443 \frac{e\lambda F}{k_B} \cdot \sqrt{\frac{M}{2m}}, \quad (5)$$

where  $m$  is electron mass and  $M$ , the molecular mass.

Druyvesteyn distribution is expressed as

$$f_D(E) = \frac{2e}{\Gamma(3/4)} \left( \frac{3m}{M\lambda^2 e^2 F^2} \right)^{3/4} E^{1/2} \exp\left(-\frac{3mE^2}{M\lambda^2 e^2 F^2}\right), \quad (6)$$

where  $\Gamma(3/4) \simeq 1.2254$  is the gamma function. The collision frequency and the free path length of electrons are assumed to be independent of energy in Maxwell and Druyvesteyn distributions, respectively. Druyvesteyn distribution is characterized by a considerably more drastic decrease in the number of electrons in the tail than that of Maxwell distribution.

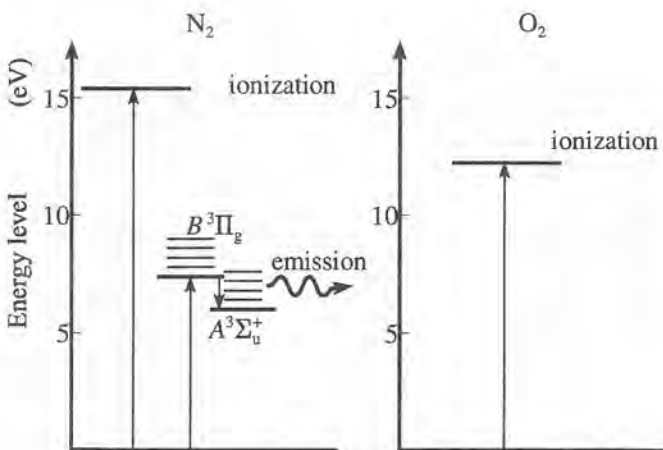


Fig. 1. A schematic drawing of  $N_2$  and  $O_2$  energy levels considered in calculation of atmospheric dark discharge luminescence by the excitation of free electrons accelerated by the seismic electric field.

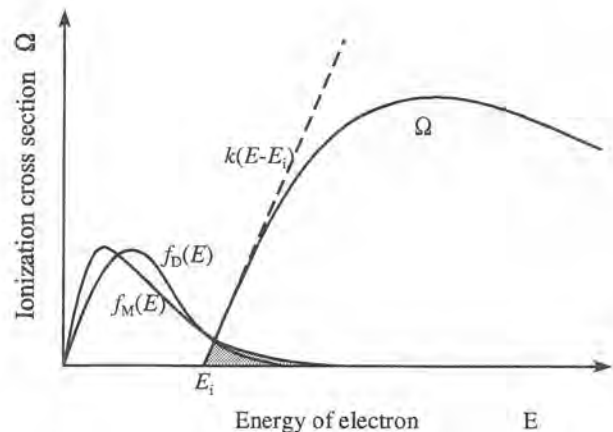


Fig. 2. The distribution of electron energy and approximation of the ionization cross section using the first order function,  $k(E - E_i)$ . Maxwell and Druyvesteyn distributions are used to estimate the electron energies under a seismic electric field. Druyvesteyn distribution,  $f_D$  is characterized by an abrupt decrease in the number of electrons in the high energy field in comparison with that of the Maxwell distribution,  $f_M$ .

Maxwell and Druyvesteyn distributions are both discussed for comparison. If Maxwell electron energy distribution is used,  $\nu_i$  becomes for  $N_g k = a_0(273/T_g)p$  and so,

$$\nu_i = a_0 \left(\frac{273}{T_g}\right) p \left(\frac{8e}{\pi m}\right)^{1/2} E_i^{3/2} \left(\frac{k_B T_e}{e E_i}\right)^{1/2} \left(1 + \frac{2k_B T_e}{e E_i}\right) \exp\left(-\frac{e E_i}{k_B T_e}\right), \quad (7)$$

where  $p$  and  $a_0$  are pressure and the ionization rate constant, respectively. In the air,  $a_0$  is  $0.26 \text{ cm}^{-1} \cdot \text{V}^{-1} \cdot \text{Toll}^{-1}$ . The values of  $E_i$  for nitrogen and oxygen gases are 15.5 eV and 12.2 eV, respectively.<sup>11)</sup>

When Druyvesteyn distribution is used, eq. (2) becomes

$$\nu_i = a_0 \left(\frac{273}{T_g}\right) p \sqrt{\frac{2e}{m}} \cdot \frac{2}{\Gamma(3/4)} \left(\frac{3m}{M\lambda^2 e^2 F^2}\right)^{3/4} \int_{E_i}^{\infty} E(E - E_i) \exp\left(-\frac{3mE^2}{M\lambda^2 e^2 F^2}\right) dE. \quad (8)$$

The frequencies of electron attachments in dry air,  $\nu_a$ , are given by the attachment probabilities of electrons,  $h$  measured at the field more than  $4 \times 10^4 \text{ V/m}$ <sup>13)</sup> using  $\nu_a = hu_c/\lambda$ . Numerical calculations of the ionization frequency were made using eqs. (7) and (8) on the condition at the ground surface, i.e.,  $T_g = 300 \text{ K}$  and  $p = 1 \text{ atm}$ .

Figure 3 shows the frequencies of electron attachments in dry air and of ionization in nitrogen and oxygen gases in the case of Maxwell and Druyvesteyn distributions. The electric field intensity where the ionization frequency is higher than that of the attachment would be more than  $6 \times 10^4$  and  $1.5 \times 10^5 \text{ V/m}$  in gaseous nitrogen for the Maxwell and the Druyvesteyn distributions, respectively. Ionization of  $N_2$  proceeds above these electric field intensities, leading to the multiplication of electrons in the atmosphere.

### 2.3 Estimation of a luminous area

Free electrons accelerated by the field may excite  $N_2$  and  $O_2$  molecules directly to the excited states without ionization.

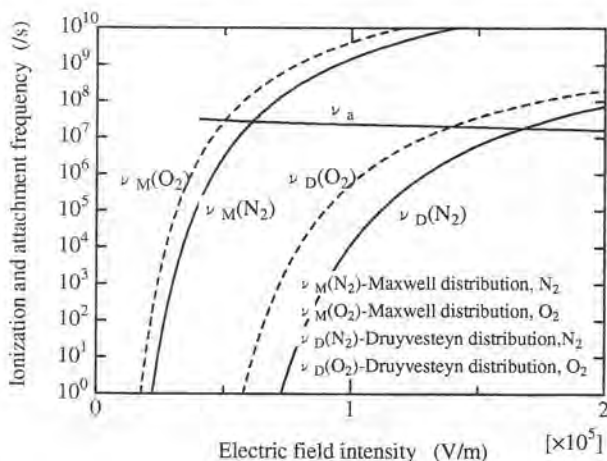


Fig. 3. Attachment frequency of electrons in dry air,  $\nu_a$  and ionization frequency in nitrogen,  $\nu(N_2)$  and oxygen,  $\nu(O_2)$  gases. The subscripts M and D are related to the Maxwell and the Druyvesteyn distributions, respectively. The electric field intensity where the ionization frequency is higher than that of the attachment is more than  $6 \times 10^4$  and  $1.5 \times 10^5 \text{ V/m}$  in nitrogen gas for the Maxwell and the Druyvesteyn distributions, respectively.

However, the number of excited molecules can be negligible small in a weak electric field as most electrons are attached to the molecules before excitation as shown in Fig. 3. In this respect, the luminous EQL area was overestimated in our former work.<sup>14)</sup> The EQL area was estimated in this work assuming that EQL is produced by ionization in the electric field range where the ionization frequency is higher than that of the attachment. Electrons excite  $N_2$  molecules to the level of  $B^3\Pi_g$  and the transition to the lower state,  $A^3\Sigma_u^+$ , occurs following the emission of light. The luminous area was calculated from eq. (1) on the condition that the area is in the electric field range, where  $\nu_i$  in gaseous nitrogen is higher than  $\nu_a$  in dry air. Only  $N_2$  excitation is considered in this work because the glow discharge in the air makes no spectral line corresponding to  $O_2$ .

The electric field in the air was estimated considering the appearance of transient charges caused by the change of seismic stress,  $\sigma$ , and the decay of the change in a conductive earth with the dielectric constant,  $\epsilon$ , and the resistivity,  $\rho$ . The charges,  $q$  may be expressed as

$$\frac{dq}{dt} = -\alpha \left(\frac{d\sigma}{dt}\right) - \frac{q}{\epsilon\rho}, \quad (9)$$

where  $\alpha$  is the piezoelectric coefficient.<sup>14)</sup> These charges cause the electric field in the air. An earthquake model derived by considering the stress drop,  $\Delta\sigma$ ,<sup>15)</sup> gives the stress change as,  $\sigma(t) = \Delta\sigma \exp(-t/\tau)$ . The charge density was obtained from eq. (9), and is expressed as

$$q(t) = \alpha\Delta\sigma \frac{\epsilon\rho}{\tau - \epsilon\rho} \times \left\{ \exp\left(-\frac{t}{\tau}\right) - \exp\left(-\frac{t}{\epsilon\rho}\right) \right\}, \quad (10)$$

The charge relaxation time for electrostatic processes is  $\epsilon\rho = 0.7 \mu\text{s}$  for a typical value of  $\epsilon = 8\epsilon_0$  and  $\rho = 10^4 \Omega\text{m}$  in granite. The piezoelectric coefficient is  $4.6 \times 10^{-12} \text{ C/N}$  for quartz crystal in shear stress. The charge density was calculated using eq. (10) for the piezoelectric constant of quartz crystal, the dielectric constant and the resistivity of granite.

Figure 4 shows the time dependence of the charge density and the electric field intensity on the ground zone due to seismic stress change for a local fracture of the quartz grain size. The intensity of electric field rises in the time of  $\epsilon\rho$  and decays in the displacement time of  $\tau$  which is on the order of  $\mu\text{s}$ . The maximum charge density,  $q_{\text{max}}$ , is given as

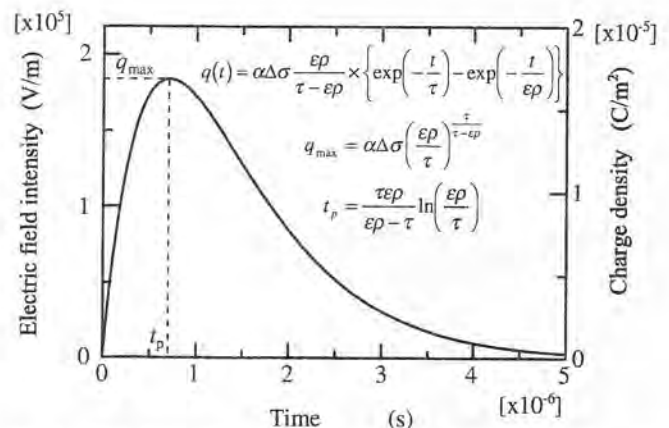


Fig. 4. Time dependence of the charge density and the intensity of electric field on the ground for a local fracture of the quartz grain size with an effective stress drop of  $\Delta\sigma = 10^7 \text{ N/m}^2$ .

$$q_{\text{max}} = \alpha \Delta \sigma \left( \frac{\epsilon \rho}{\tau} \right)^{\frac{r}{r-\epsilon \rho}} \quad (11)$$

The electric field is more than  $1.5 \times 10^5$  V/m on the fault. The charge density would be enhanced if a large quartz vein existed under the ground. If a new physical process of ferroelectric orientation of piezo-compensating, bound charge pairs were present, an intense charge density will be produced.<sup>16)</sup>

A luminous area was estimated assuming the charges produced by seismic stress change for a local, 10-m-long fracture. The charges were approximated for the charge densities of  $q = 1.0 \times 10^{-5}$  C/m<sup>2</sup> in the area of  $10 \times 10$  m during  $2.0 \times 10^{-6}$  s in the calculation considering Fig. 4. We considered the sum of charges induced in sequence. Charge sustenance time on the order of  $\mu$ s is sufficiently long for ionization to occur because electrons are accelerated to 94% of the final velocity within  $10^{-8}$  s. The field intensity in the air is given for the charge  $q$  in the soil as,

$$F(x, y, z) = \frac{1}{4\pi\epsilon} \cdot \frac{2\epsilon}{\epsilon + \epsilon_0} \iint_x \frac{q}{(x-x_1)^2(y-y_1)^2z^2} dx_1 dy_1 \quad (12)$$

The charge  $-q$  was simply assumed at another edge of the fault segment. A spatial distribution of EQL was calculated from  $F(x, y, z)$  assuming Maxwell distribution of the electron energy as shown in Fig. 5(a). The shape of the EQL in this calculation is similar to that photographed during the Matsushiro Earthquake.<sup>1)</sup>

### 2.4 Estimation of luminous intensity

Luminous intensity was calculated using the above conditions considering the atmospheric polarization and the emission of light from the  $B^3\Pi_g$  excitation energy level of  $N_2$  molecules as shown in Fig. 1. A nitrogen molecule in the excited state emits a band spectrum around 650 nm in the transition to the metastable state of  $A^3\Sigma_u^+$ .<sup>17)</sup> Electron multiplication followed by subsequent ionizations would occur in earthquake lightning. The density of the free electrons may be described as

$$n(z, t) = \frac{\Delta n_r}{v_i(z) - v_a(z)} [\exp\{(v_i(z) - v_a(z))t\} - 1] \quad (13)$$

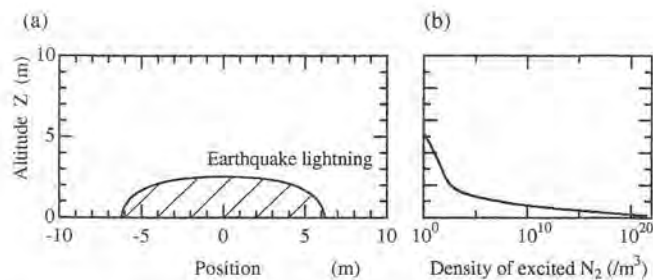


Fig. 5. (a) Spatial distribution of EQL calculated assuming the Maxwell distribution of the electron energy using the pulse charge density,  $q$ , of  $10^{-5}$  C/m<sup>2</sup> at the area of  $10 \times 10$  m. The charge  $-q$  was simply assumed at another edge of the fault segment. The EQL zone is shaped like a dome of light, similar to that photographed during the Matsushiro earthquakes. (b) The altitude ( $z$ ) dependence of the density of excited  $N_2$  molecules on the center of the area where the charge appears.

The accelerated free electrons produce the excited molecules until the charges at the epicenter are compensated by free charges. The time,  $T$ , required for the electric field canceled by the polarization was estimated using the drift velocity of electrons,  $u_d(z) = (e/m)^{1/2}(m/M)^{1/4}(F(z)\lambda(z))^{1/2}$ , assuming that the electric field is constant, and is expressed as

$$\int_0^T n(z, t) u_d(z) dt = q \quad (14)$$

The excitation frequency of  $N_2$  molecules,  $\nu_e$  is given as

$$\nu_e = N_N \int_0^\infty \Omega_N(u_e) u_e f(u_e) du_e \quad (15)$$

where  $N_N$  and  $\Omega_N$  are the density of  $N_2$  molecules and the excitation cross section of  $B^3\Pi_g$ .<sup>12)</sup> The density of excited  $N_2$  molecules,  $N_e$  was calculated on the condition of  $T$  obtained by eq. (14) as

$$N_e(z) = \int_0^T n(z, t) \nu_e(z) dt \quad (16)$$

The altitude ( $z$ ) dependence of the density of excited  $N_2$  molecules is shown in Fig. 5(b). The emission intensity is estimated at  $3 \times 10^{20}$  photons/m<sup>3</sup> close to the fault zone for an assumed quantum efficiency of 10%. The total number of photons entering a 1 cm<sup>2</sup> area are about  $3 \times 10^{10}$  at a distance 1 km away from the fault zone. The illuminance is 0.1 lux at a distance 1 km away from the luminous area considering the visibility factor at 650 nm and the afterimage time of the naked eye at 0.1 s. This flash of light is sufficiently intense to be visible even under a full moon.

The charge distribution and the inhomogeneity of the field would presumably lead to the different shapes of EQL reported for different earthquakes. Sometimes, a ball-like EQL was observed to be moving rapidly. The area of the pulsed charge appearance might be moving at a speed close to the S wave (3.5 km/s) as the rupture proceeds along the fault leading to stress release at the fault zone.

Ionization which causes EQL might form fog or clouds if the atmosphere is supercooled as to allow the ionization and the subsequent formation of nucleus for moisture precipitation. This was also demonstrated experimentally using a Van de Graaff electric generator in a preliminary report.<sup>3)</sup> Details on cloud formation by an electric field will be discussed separately, elsewhere.

### 3. Summary

A model of the "dark discharge" caused by ground charges temporally induced by seismic fault movements was proposed to explain the electroatmospheric phenomenon of earthquake lightning. The charges released from the piezoelectric polarization of quartz grains produce a pulsed electric field of more than  $1.5 \times 10^5$  V/m on the fault zone. The electric field in the air accelerates free electrons in atmosphere. Both Maxwell and Druyvesteyn distributions of the electron energy under the field were used to estimate the ionization and excitation of  $N_2$  and  $O_2$  molecules. The spatial distribution of EQL is similar to a shape of the dome photographed during the Matsushiro Earthquake. An illuminance of 0.1 lux can be observed 1 km away from the luminous dome and be visible under a full moon.

- 1) Y. Yasui: Mem. Kakioka Magn. Obs. **13** (1968) 25.
- 2) K. Wadatsumi: *Zenchou Shogen 1519* (1519 Witnessed Phenomena Prior to Earthquake) (Tokyo Pub., Tokyo, 1995) [in Japanese].
- 3) M. Ikeya: *Jishin no Mae, Naze Dobutsu ha Sawagunoka* (Why Do Animals Behave Unusually before an Earthquake) (NHK Press, Tokyo, 1998) [in Japanese].
- 4) H. Tributsch: *When the Snakes Awake* (MIT Press, Boston, 1982).
- 5) B. T. Brady and G. A. Roswell: Nature **321** (1986) 488.
- 6) A. C. Johnston: Nature **354** (1991) 361.
- 7) T. Terada: Bull. Earthquake Res. Inst., Univ. Tokyo **9** (1931) 225.
- 8) H. Mizutani, T. Ishido, T. Yokokura and S. Ohnishi: Geophys. Res. Lett. **3** (1976) 365.
- 9) D. Finkelstein, R. D. Hill and J. R. Powell: J. Geophys. Res. **78** (1973) 992.
- 10) A. A. Radzig and B. M. Smirnov: *Reference Data on Atoms, Molecules, and Ions* (Springer-Verlag, Berlin, 1985).
- 11) A. von Engel: *Ionized Gases* (Oxford University Press, Oxford, 1955).
- 12) Y. P. Raizer: *Gas Discharge Physics* (Springer-Verlag, Berlin, 1991).
- 13) S. Takeda: *Kitai Hoden no Kiso* (Basis of Gas Discharge) (Tokyo Electrical Machinery University Press, Tokyo, 1990) [in Japanese].
- 14) M. Ikeya and S. Takaki: Jpn. J. Appl. Phys. **35** (1996) 355.
- 15) J. N. Brunc: J. Geophys. Res. **75** (1970) 4997.
- 16) M. Ikeya, H. Sasaoka, K. Teramoto and C. Huang: Ionics **23** (1997) Suppl. **2**, p. 3.
- 17) G. Herzberg: *Spectra of Diatomic Molecules* (Van Nostrand Reinhold, New York, 1950) 2nd ed.